11-2011

Consistency in statistical moments as a test for bubble cloud clustering

Thomas C. Weber
University of New Hampshire, Durham, thomas.weber@unh.edu

Anthony P. Lyons
Pennsylvania State University - Main Campus

David L. Bradley
Pennsylvania State University - Main Campus

Consistency in statistical moments as a test for bubble cloud clustering

Thomas C. Weber[a)]
Center for Coastal and Ocean Mapping, University of New Hampshire, 24 Colovos Road, Durham, New Hampshire 03824

Anthony P. Lyons and David L. Bradley
Applied Research Laboratory, Pennsylvania State, State College, Pennsylvania 16804-0030

(Received 1 December 2010; revised 11 August 2011; accepted 15 August 2011)

Frequency dependent measurements of attenuation and/or sound speed through clouds of gas bubbles in liquids are often inverted to find the bubble size distribution and the void fraction of gas. The inversions are often done using an effective medium theory as a forward model under the assumption that the bubble positions are Poisson distributed (i.e., statistically independent). Under circumstances in which single scattering does not adequately describe the pressure field, the assumption of independence in position can yield large errors when clustering is present, leading to errors in the inverted bubble size distribution. It is difficult, however, to determine the existence of clustering in bubble clouds without the use of specialized acoustic or optical imaging equipment. A method is described here in which the existence of bubble clustering can be identified by examining the consistency between the first two statistical moments of multiple frequency acoustic measurements. © *2011 Acoustical Society of America*. [DOI: 10.1121/1.3636369]

PACS number(s): 43.30.Ft, 43.30.Es, 43.30.Pc [TGL] Pages: 3396–3405

I. INTRODUCTION

The effect of gas bubbles on small amplitude sound waves propagating in fluids has been well studied, beginning with Mallock's "frothy water" (Mallock, 1910) and developing into an applied research topic as naval researchers began to understand the strong signature of bubbles in ship wakes (NDRC, 1946) and oceanographers developed an appreciation for the importance of bubbles in a variety of phenomena, especially near surface wind-wave interaction (e.g., Thorpe, 1982). The theories that have been set forth and widely used are typically effective medium theories which treat two-phase bubbly mixtures as a single, homogenized medium with characteristics describing the average propagation (e.g., Foldy, 1945; Van Wijngaarder, 1972; Commander and Prosperetti, 1989).

Foldy (1945) developed an effective medium solution by considering multiple scattering, where the incident field at each bubble includes contributions from every other bubble. Our interpretation of Foldy's result—upon which the work herein depends, and upon which the literature can occasionally be confusing—is that it incorporates one-way multiple scattering as defined by Ye and Ding (1995, section 1A, and Fig. 1). One-way multiple scattering includes those waves that have interacted with two or more scatterers, except where the wave interacts with any individual scatterer twice. Or, in the words of Kargl (2001), "the scattered field from a given scatterer can interact with one or more new scatterers in the distribution, but a portion of this scattered field cannot return to any previously visited scatterer." Hahn (2007) uses the same definition when describing Foldy's result, although he also somewhat ambiguously includes a description of one-way multiple scattering as neglecting "backscatter" between scatterers (for isotropic scatterers, at least, one-way multiple scattering would include portions of scattering "chains" for which the scattered field is propagating back toward the source prior to interaction with another scatterer).

Most recently, the equivalence of Foldy's result to one-way multiple scattering has been shown by both Ye and Ding (1995) and Henyey (1999) using diagrammatic techniques. An analogous expansion of the multiple scattering series into successive orders of scattering and re-derivation of Foldy's work also appears in Weber (2008, equations 12–14). Weber (2008) do not specifically discuss one-way multiple scattering in their brief derivation, but it is worth noting that in their expression for triple scattering the ensemble average is explicitly computed over three *assumed independent* bubbles rather than two independent bubbles, one of which is revisited, which is essentially the same conclusion that can be found in Twersky (1953, section 3.3). Further, numerical simulations by Weber *et al*. (2007a Fig. 5) demonstrate the differences between the single scatter solution, the single plus double scatter solution, and Foldy's approximate result, indicating that Foldy's approximate solution incorporates more than just single scattering.

Several authors including Ye and Ding (1995), Henyey (1999), and Kargl (2001) have discussed corrections to Foldy's approximate solution with the goal of incorporating the missing scattering contributions, likely to become important near resonance for high void fractions [e.g., void fractions greater than 1.0×10^{-4} for the Gaussian bubble size distributions examined by Kargl (2001)]. It is assumed that

a)Author to whom correspondence should be addressed. Electronic mail: weber@ccom.unh.edu

for the bubble clouds considered in the present work, which have void fractions that are approximately 1.0×10^{-6} or lower, albeit with non-Gaussian shaped bubble distributions, any corrections that extend Foldy's multiple scattering solution beyond one-way multiple scattering are negligible.

In addition to the approximation leading to one-way multiple scattering, Foldy (1945) also assumed that the probability of a bubble being located at some particular location within a bubble cloud with a given scattering amplitude s was independent of the locations and scattering amplitudes of any other bubble. This assumption may break down within a cloud of bubbles when the bubbles are clustered, or, using the terminology of Eaton and Fessler (1994), preferentially concentrated. In the context of this work, clustering can only be defined using multipoint statistics. For example, the average bubble number density n (a single point statistic) can vary in space across, for example, a ship wake or a breaking wave bubble plume, a scenario that is readily handled by the effective medium theories of Foldy (1945), Commander and Prosperetti (1989), and others. Clustering, however, *is* present in a bubble cloud when the joint probability density function (pdf) describing the simultaneous locations of two bubbles is not equal to the product of the marginal pdfs describing the locations of the individual bubbles. For very dense clouds of scatterers, clustering takes the form of a "hole correction" which represents the impossibility of two scatterers occupying the same location (Fikioris and Waterman, 1964). This effect, which results in a stochastic dependency in bubble positions over distances on the order of a bubble diameter, is likely to be negligible for bubble clouds of interest in, for example, the ocean. However, it is conceivable that bubbles can also become clustered on longer scales. This may occur when bubbles interact with turbulent flows, either because they cross streamlines in a similar fashion to the small particles described by Eaton and Fessler (1994) or because the average bubble number density (a single point statistic) exhibits a spatial gradient that causes the entrainment of bubble-rich fluid into bubble-poor fluid (or vice versa). In both of these examples the clustering is occurring on the interior of a bubble cloud, and this is the scenario that will be considered herein.

The effect of bubble clustering on acoustic propagation has been examined by Weber *et al.* (2007a,b) and Weber (2008) who treated the interaction between the acoustic waves and bubbles using Foldy's (1945) classic multiple scattering approach and found that clustering changes both the attenuation of the average acoustic pressure field and the higher order statistical moments. If bubble clustering is unaccounted for when it is present, it can lead to erroneous performance predictions for sonar systems in a ship wake or near the ocean surface under breaking waves, and errors in the estimation of bubble number density and void fraction when inverting acoustic data (attenuation and/or sound speed) for oceanographic purposes.

Without the use of specialized high frequency acoustic or optical imaging equipment it is often difficult to determine if bubble clouds are clustered. The goal of this paper is to describe an alternative method for identifying the impact of bubble clustering on multiple frequency acoustic measurements by examining the consistency between the first two statistical moments of the measurements themselves. This method is based on the results presented in Weber *et al.* (2007a) that showed that clustering tended to lower the attenuation of the average acoustic field (a first moment quantity) while increasing the variance for the scenario they were examining. In scenarios where multifrequency measurements of the average attenuation and/or sound speed are made for the purposes of inverting for bubble size distribution (e.g., Medwin, 1977; Lamarre and Melville 1995), the contrasting behavior between the first two statistical moments can be utilized to determine when clustering is present. This idea has been discussed previously by Weber *et al.*, (2007b), and is further developed and demonstrated here with a laboratory experiment in which both clustered and nonclustered bubble clouds were generated.

II. CONSISTENCY BETWEEN THE 1ST AND 2ND MOMENTS

Predictions of the acoustic pressure field p at some field point $\vec{r}$ in the presence of bubbles can be made using Foldy's multiple scattering approach (Foldy, 1945) which starts with a set of coupled equations:

$$p(\vec{r}) = p_o(\vec{r}) + \sum_i s(a_i) p^i(\vec{r}_i) G(\vec{r}, \vec{r}_i),$$
$$p^i(\vec{r}_i) = p_o(\vec{r}_i) + \sum_{i' \neq i} s(a_{i'}) p^{i'}(\vec{r}_{i'}) G(\vec{r}_i, \vec{r}_{i'}), \quad (1)$$

where p_o is the pressure field that would be observed in the absence of any bubbles, s is the complex scattering coefficient for the ith bubble with radius a_i, G represents the free-space Green's function for a point source, and p^i represents the incident field at a bubble. These equations are exact for a particular configuration of bubbles, more generally they are ensemble averaged over all possible configurations (realizations) of the bubble cloud to yield the average pressure field. The positions of each bubble are treated as random variables, and the ensemble average can be explicitly found using the joint pdf $\rho(\vec{r}_1, \vec{r}_2, \vec{r}_3, \ldots)$ describing the positions of each of the bubbles within the bubble cloud. Foldy (1945) made the assumption that the positions of each bubble were independent random variables, in which case the joint pdf was equal to the product of marginal pdfs. This simplifying assumption ultimately leads to a complex effective medium wavenumber k describing both the attenuation and dispersion in the average pressure field:

$$k^2 \cong k_o^2 + 4\pi \int_o^\infty s(a) n(a) da = k_o^2 + 4\pi S, \quad (2)$$

where k_o is the wave number for the bubble free fluid, and $n(a)$ is the bubble size distribution. This effective medium wave number is complex and describes both the attenuation and dispersion in the bubbly fluid.

Weber (2008) considered the case where clustering was present, i.e., the assumption that the bubble positions are statistically independent no longer holds true. By treating the

statistics of the bubble cloud using a quasicrystalline approximation similar to that used by Lax (1952) for very densely packed scatterers, a correction term for Eq. (2) was developed:

$$k^2 \cong k_o^2 + 4\pi S + 4\pi S^2 \langle p(\vec{r})\rangle^{-1} \times \int_V p_o(\vec{r}_i) G(\vec{r}_i, \vec{r})[g(|\vec{r}_i - \vec{r}|) - 1] n(\vec{r}_i) d\vec{r}_i \quad (3)$$

where $\langle p(\vec{r})\rangle$ denotes the ensemble average of $p(\vec{r})$. The last term on the right-hand side is the correction term, which utilizes the pair correlation function, g, to relate the joint pdf function to the marginal pdfs for each bubble:

$$n(\vec{r}_i, \vec{r}) = n(\vec{r}_i) n(\vec{r}) g(|\vec{r}_i - \vec{r}|). \quad (4)$$

The correction term in Eq. (3) vanishes when either clustering is not present, in which case the pair correlation function, g, is equal to 1, or when single scattering adequately describes the acoustic field. As described in Weber *et al.* (2007a), the latter can happen because the scatterers are weak, the bubble cloud is small, the propagation distance through the bubble cloud is small, or some combination of the three.

Equations (2) and (3) are derived by ensemble averaging the acoustic pressure field, and consequently are first statistical moment quantities. Observations of acoustic fields in the presence of random clouds of scatterers can also fluctuate, and these fluctuations can be examined by considering the variance in the acoustic field, which is (Ishimaru, 1978, see eq. 14–28)

$$\langle p(\vec{r}) p^*(\vec{r})\rangle - \langle p(\vec{r})\rangle \langle p^*(\vec{r})\rangle = \int_V \int s_i s_i^* \langle p(\vec{r}_i) p^*(\vec{r}_i)\rangle G_e(\vec{r}, \vec{r}_i) \times G_e^*(\vec{r}, \vec{r}_i) n(\vec{r}_i, a_i) da_i d\vec{r}_i, \quad (5)$$

where G_e is the effective medium wavenumber and is identical to G but uses the effective medium wavenumber k rather than k_o.

When clustering is present and single scattering does not adequately describe the acoustic field, inversions of frequency dependent estimates of the attenuation or sound speed using Eq. (2) will be in error. It is difficult to know from observations of attenuation or sound speed alone that clustering is present and effecting the acoustic field. However, if it is assumed that the inversion is correct, then it can be used to predict the higher order statistics in the acoustic field, such as the second moment described by Eq. (5). If this same higher order statistic is estimated from the data itself, then the match between that statistic and the prediction from Eq. (5) provides a metric for determining whether clustering can be neglected and also whether Eq. (2) adequately describes the average acoustic pressure field. That is, the consistency between the 1st moment (the attenuation or sound speed characterizing the average pressure field) and the 2nd moment (the average intensity in the pressure field) can be used to provide a metric for determining whether the clustering is having a nonnegligible impact on the acoustic field.

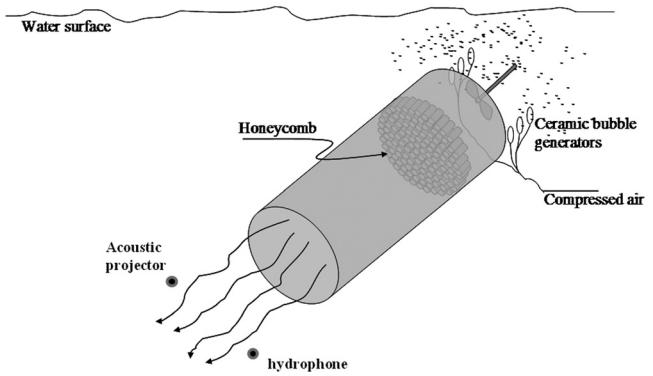

FIG. 1. Experimental setup.

III. A LABORATORY EXAMPLE

In order to illustrate and verify the first/second moment consistency method for identifying the effects of bubble clustering, a laboratory apparatus was constructed to create both clustered and nonclustered bubble clouds. The laboratory measurements were conducted in an 8.7 m long, 6.9 m wide, and 5.5 m deep tank of water at the Penn State Applied Research Laboratory. Bubbles were generated using several cylindrical pieces of porous ceramic connected to a pressurized air supply. These devices were originally designed to extract water from soil (they are called Remote Soil Water Samplers) and are 6 cm long hollow ceramic rods that are closed on one end. The end that is not closed is fitted with a tube so that a gas can be pumped through the ceramic, creating bubbles. These same devices have also been used to create bubbles by Coakley *et al.* (2002) who quote a maximum pore size in the ceramic of 2.5 μm. Coakley *et al.* (2002) generated nitrogen bubbles in a 25.4 cm cylindrical glass beaker, allowing the large bubbles emitted from the ceramic to rise to the surface while small bubbles were distributed throughout the volume using a magnetic stirrer. They then measured the bubble size distribution using a laser *in situ* scattering and transmissometry (LISST) instrument (Agrawal and Pottsmith, 2000), finding a distribution of bubble radii that ranged from 15–55 μm with a mean of approximately 30 μm. From the standpoint of acoustic inversion for oceanic bubble size distributions this size range is attractive as large numbers of bubbles in this size range are often found under breaking waves (e.g., Johnson and Cooke, 1979).

In the experiments that are of interest here, the newly created bubbles were generated just outside of a 2 m long, 0.5 m diameter duct near a propeller (Fig. 1). The propeller, which was attached to a variable speed motor, was used to create a flow of water though the duct into which the bubbles were entrained. By placing the bubble generators just outside the inlet, the larger bubbles were able to freely rise to the surface while the smaller bubbles (whose buoyant rise speeds are smaller) were entrained in the flow through the duct. This was done to limit the acoustic frequencies required to characterize the bubble population, which is

done by measuring the frequency dependent attenuation (to be discussed below). There was some concern that high levels of vorticity in the flow downstream of the propeller would impose a fluctuating spatial structure (i.e., clustering) on the bubble cloud that was being swept down the duct. To mitigate this effect, a honeycomb of 12.7 cm long by 3.81 cm diameter PVC tubes was stacked into the duct in order to straighten the swirling flow. Similar strategies have been employed in wind tunnels, although flow straightening vanes are perhaps more common (Barlow *et al.*, 1999). In addition to reducing the vorticity in the propeller driven flow, it was also hoped that the honeycomb structure would serve to spatially mix the bubble flow downstream as the jets of water exiting the PVC tubes interacted with each other in a similar fashion to what might be expected for grid generated turbulence (Mehta and Bradshaw, 1979). Acoustic propagation measurements were conducted just downstream of the duct exit (1.63 m downstream of the honeycomb structure).

In order to determine the applicability of the theory describing acoustic propagation through nonclustered bubble clouds to the bubble cloud generated by the apparatus shown in Fig. 1, it was necessary to measure the structure (or the lack of structure) in the bubble cloud. This was done using a Reson 8101 multibeam sonar. This sonar operates at a center frequency of 240 kHz and transmits short pulses from a line array with a beam pattern that is nominally $1.5^\circ \times 170^\circ$. Backscattered acoustic signals are received on 101 identical $15^\circ \times 1.5^\circ$ beams that are oriented to make measurements in a plane over a 150° arc. Using the product theorem (Kinsler *et al.*, 2000), the combination of transmit and receive arrays results in beams that are $1.5^\circ \times 1.5^\circ$.

The multibeam sonar was located beneath the duct looking upwards, and used to make measurements of a cross-section of the bubble plume in a plane that was orthogonal to the direction of the flow, approximately 0.3 m downstream of the exit of the duct and approximately 1.4 m below the midpoint of the duct. The raw data output from the multibeam sonar processor consists of the 101 beam time series, each of which is sampled at 15 ksamples/s. The spatial distribution of the average backscatter from 300 pings of multibeam data—a proxy for the bubble number density, and a single-point statistic that does not in itself provide information regarding the presence of clustering—is shown in Fig. 2. The shape of the jet of bubbles exiting the duct can clearly be seen, as can the effect of bubble buoyancy which is manifested as an increase in the bubble number density above the jet and the relatively small amount of bubbles found below the jet.

The multibeam sonar data can also be used to estimate the pair correlation function g in the bubble cloud using the methodology described by Weber (2008), where the pair correlation estimate was given as

$$g(|\vec{r}_1 - \vec{r}_2|) = \frac{\langle p_1(\vec{r}_1) p_2^*(\vec{r}_2)\rangle}{\langle p_1(\vec{r}_1)\rangle \langle p_2^*(\vec{r}_2)\rangle}. \quad (6)$$

In Eq. (6), p_1 and p_2 are measurements proportional to the acoustic pressure that are directly recorded from the multibeam sonar. As in Weber (2008), it is assumed that the multibeam measurements are at sufficiently high frequency (and hence off resonance for most bubbles) that only single scattering is important. Equation (6) was estimated from the same 300 pings used to generate the average bubble density at ranges $r = |\vec{r}_1 - \vec{r}_2|$ varying from 3–50 cm, with the result (solid line) shown in Fig. 3. Individual estimates of Eq. (6) are found by computing a time average over the 300 pings for individual pairs of multibeam resolution "cells" (see Fig. 2), each of which is shown in Fig. 3 in order to provide an estimate of the range of the data. These data are binned at a resolution of 0.02 m, and then each bin is averaged in order to provide the final pair correlation estimate. The standard deviation in the pair correlation estimate for each bin is between 0.03 and 0.04 at ranges between 0.06 and 0.5 m, and there are more than 100 measurements in each of these bins. Note that by replacing the ensemble average in Eq. (6) with an average across time, the random processes governing the bubble cloud have been assumed to be ergodic. Inherent in this assumption is that these random processes are stationary, a condition that is more easily achieved in the controlled conditions of a laboratory setting than in many other settings (e.g., a bubble cloud under a breaking wave). It is also worth noting that while estimates of Eq. (6) were constrained to the plume proper (i.e., between the locations of locations of projector and hydrophone shown in Fig. 2), any variation in Eq. (6) that might exist as a function of position within the jet has been neglected.

The pair correlation estimated from the 300 pings (Fig. 3) is close to one everywhere, indicating that there is little clustering present in the bubble cloud. The notable exception to this is the increase in the pair correlation at distances less than 6 cm, where a maximum pair correlation of 1.175 is reached. The data at these short distances comes from adjacent beams which overlap each other at the half-power (−3 dB) points, making it likely that the apparent increase in pair correlation for adjacent beams is an artifact of the system.

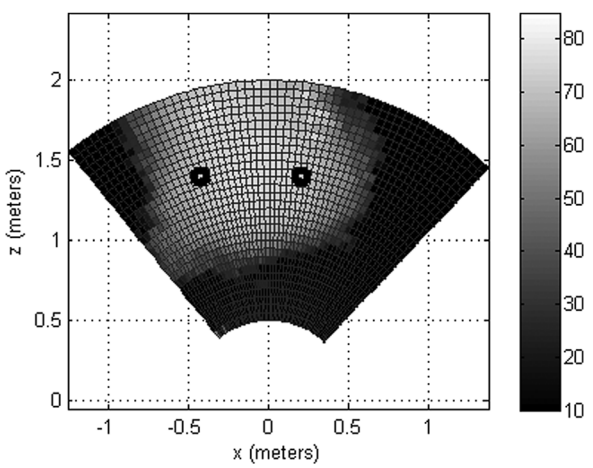

FIG. 2. The average multibeam backscatter from the bubble cloud (in dB, relative units), representing the spatial dependence of the average bubble number density. The two circles represent the location of the projector and the hydrophone used in the propagation experiment, which are located at a height corresponding to the midpoint of the circular duct in which the bubbles were generated. The solid lines represent the spatial resolution of the multibeam as a function of both beam angle and range.

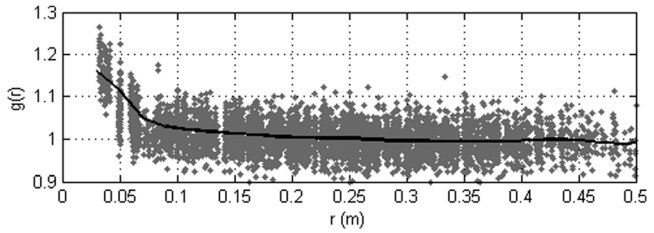

FIG. 3. The pair correlation function for the assumed nonclustered bubble cloud, including individual estimates (dots) from the various pairs of multibeam resolution cells and their combined average (solid line).

At the same time that the multibeam sonar data shown in Figs. 2 and 3 were being collected, 0.2 ms long gated cw pulses were transmitted through the bubble cloud across a 0.57 m long path from a fixed source to a fixed receiver at the locations shown in Fig. 2. Nine different signals corresponding to frequencies of 15, 25, 35, 43, 51, 59, 68, 80, and 120 kHz were transmitted across the bubble plume, each of which had a bandwidth of ~5 kHz. These signals were transmitted from an Agilent 33120A signal generator, amplified on a Krohn-Hite 7500 power amplifier, and then transmitted into the water from an ITC-1042B spherical transducer at source levels less than 170 dB re 1 μPa at 1 m. The entire sequence of 0.2 ms signals was transmitted in less than 10 ms, and the sequence was staggered in frequency (15, 43, 68, 25, 51, 80, 35, 59, 120 kHz) in order to keep the frequency difference between adjacent pings large so that interference caused by the pulse reverberating from the mechanical elements of the experiment was reduced. After propagating through the bubble cloud, the signal was received on a Reson TC4042 spherical hydrophone, amplified and filtered using a Krohn-Hite model 3364 filter, and then digitized at a rate of 333 ksamples/s and at a resolution of 16 bits.

The pulse train was transmitted 20 times per second for up to 5 min in order to generate a statistically significant ensemble of propagation data through the bubble cloud. The signal amplitudes were extracted in the frequency domain, and then compared to the amplitudes received when no bubbles were present in order to estimate the frequency dependent attenuation, which is shown in Fig. 4. Note that for the case where no bubbles were present, the signal amplitudes represent the scenario where the air supply attached to the bubble generators was switched off, but the air motor was still running. Tests done for this no-bubble scenario show that the variance of the signal amplitude was less than 0.1% of the squared mean signal amplitude for all frequencies. The maximum attenuation observed here is 3.9 Nepers/m (33.9 dB/m) at frequency of 35 kHz. This attenuation curve has been inverted to find the bubble size distribution $n(a)$ using the iterative technique described by Caruthers *et al.* (1999), a method that utilizes Eq. (2) and inherently assumes that clustering is not present, with the result shown in Fig. 4. The data indicate a bimodal distribution of bubbles, with one size group exhibiting a peak at 25 μm in close agreement with the result reported by Coakley *et al.* (2002) with the same bubble generators. The second group of bubbles exhibits a peak near 70 μm. It is not surprising that this bimodal distribution was not observed by Coakley *et al.* (2002) given that they purposely tried to eliminate the larger bubbles by allowing them to rise to the surface before starting their measurements. The mechanism behind the bimodal distribution is not known, although one possible explanation is that the two different groups are generated at different locations on the bubble generator (e.g., one along the length, and one at the cap). The average void fraction for this bubble cloud is 4.0×10^{-6}, which roughly corresponds to the void fraction that would be observed from a Gamma plume formed under an open ocean breaking wave for a wind speed of 20 m/s using the parameterization given by Novarini *et al.* (1998).

The 1st/2nd moment consistency methodology can be employed here to examine the accuracy of the inversion procedure. An example of the fluctuating pressure amplitude, P, from which the 2nd moment is estimated, is shown in Fig. 5 where it has been normalized by the pressure amplitude P_o observed with no bubbles present. Due to the time gating of the signal observed on the hydrophone that was used when calculating the observed attenuations, the acoustic pressure fluctuations shown here correspond only to the ballistic component of the acoustic pulse. Time gating is important to consider when trying to predict the variance that would be

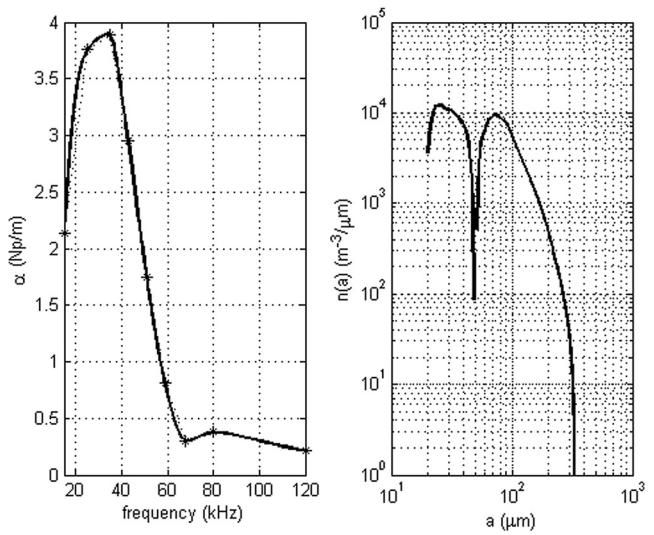

FIG. 4. A measurement of the frequency dependent attenuation (left side, stars) and the associated bubble size distribution (right side). The solid line on the left shows the attenuation that would be predicted based on (2) using the bubble size distribution from the right hand side.

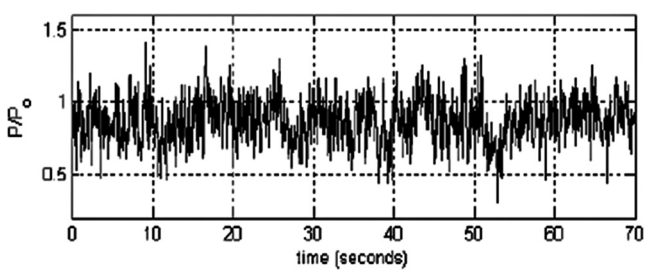

FIG. 5. An example of the observed fluctuating acoustic pressure amplitude at frrquency of 68 kHz for the open-tube setup shown in Fig. 1. The ping rate was 20 Hz, and each data point here corresponds to the amplitude of a single ping.

observed because only a portion of the bubble cloud is physically capable of contributing to the pulses. If only single scattering were important, then the region contributing to the ballistic component of the pulse via scattering would be defined by the ellipsoid shown in Fig. 6(a). If a bubble falls outside of this ellipse, then the time required for the acoustic wave to propagate from the projector to the bubble and then to the hydrophone will result in an arrival time later than the ballistic component of the pulse. For double scattering, in which an individual scattering chain contains two bubbles, the ellipse would still define the extents of the region contributing to the ballistic component, but some of the scattering chains within the ellipse would arrive later [Fig. 6(b)]. This extends to triple scattering chains, quadruple scattering chains, and so on. The difficulty in sorting out the double (or higher) scattering paths is exacerbated for very short pulses. For the experiments discussed here, the length of each pulse was 0.2 ms, which is slightly more than half the time required for the pulse to propagate from the projector to the hydrophone. Thus, most of the double scattering paths contained within the bounding ellipse will contribute to the ballistic component of the pulse.

The predicted variance is calculated by numerically evaluating an approximate form of the variance in the pressure amplitude that is found by expanding Eq. (5) and using the first two terms:

$$\begin{aligned}&\langle p(\vec{r}_i)p^*(\vec{r}_i)\rangle - \langle p(\vec{r}_i)\rangle\langle p^*(\vec{r}_i)\rangle \\ &\quad = \int_V \int s_i s_i^* \langle p(\vec{r}_i)\rangle\langle p^*(\vec{r}_i)\rangle G_e(\vec{r},\vec{r}_i) \\ &\quad \times G_e^*(\vec{r},\vec{r}_i) n(\vec{r}_i,a_i)\,da_i d\vec{r}_i.\end{aligned} \tag{7}$$

Equation (7) was evaluated with a volume integral limited to ranges for which the total path length between the source, any bubble, and the hydrophone was less than the separation distance between the source and the hydrophone plus the gated pulse length. It should also be noted that the mean pressure amplitude used in the integral is assumed to decay as $e^{-\alpha r}/r$, where α and r are the attenuation and range through the bubble cloud, respectively, as the pulse propagates away from the spherical projector. Further, the bubble size distribution is weighted so that it includes the spatially varying mean bubble size distribution shown in Fig. 2. The result of the numerical integration of Eq. (7) is shown in comparison with the observed variance (over 2000 measurements) in Fig. 7, where the variance has been normalized by the squared mean pressure:

$$\frac{\sigma^2}{\mu^2} = \frac{\langle p(\vec{r}_i)p^*(\vec{r}_i)\rangle - \langle p(\vec{r}_i)\rangle\langle p^*(\vec{r}_i)\rangle}{\langle p(\vec{r}_i)\rangle\langle p^*(\vec{r}_i)\rangle}. \tag{8}$$

The variance in the fluctuating pressure amplitude reaches a maximum of 24% of the squared mean value at 35 kHz, which is quite high considering that the acoustic pulse has traveled less than 1 m. The close match between the observed and predicted variance is an indication that bubble clustering is not present, which is expected given the pair correlation function shown in Fig. 3. The random uncertainty in the estimate of Eq. (8) from the observations includes contributions from both the estimate of the variance, σ^2, and the estimate of the squared mean, μ^2. The standard deviation in the frequency dependent estimates of Eq. (8) shown in Fig. 7 varies from approximately 5% of the estimated value for frequencies of 68 kHz and above to almost 40% at a frequency of 35 kHz, corresponding to the weakest and strongest effects of the bubble cloud on the acoustic field, respectively. Based on the consistency between the first and second moments in light of the uncertainty in these estimates, the estimated bubble sized distribution shown in Fig. 4 can be considered to be correct.

Using the same apparatus shown in Fig. 1, the consistency between first and second moments was investigated for a range of void fractions by varying the speed of the propeller which had the effect of entraining varying quantities of bubbles. Figure 8 shows the comparison between observed and predicted variance for void fractions ranging from approximately 1.1×10^{-6} to 5.8×10^{-6}, with generally good agreement. The largest deviations between the prediction and the observation appear at one of the two lowest frequencies. The reasons for these differences are not known, although one possible explanation is nonstationarity in the bubble cloud for the larger bubble sizes. Perhaps the most troubling discrepancy between observation and model in

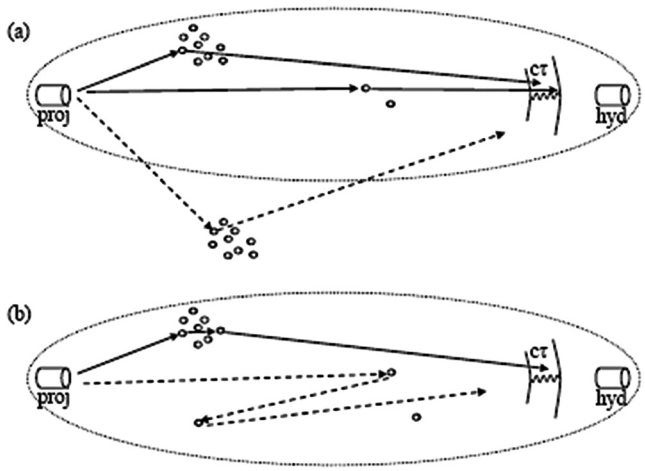

FIG. 6. The bounding ellipses for scattering contributions to the ballistic component of the acoustic pulse. The top figure shows example scattering chains that contribute to the ballistic component of the pulse (solid line) and those that arrive afterward (dashed line) for the single scattering case, and the bottom figure shows the same type of scattering for the double scattering case.

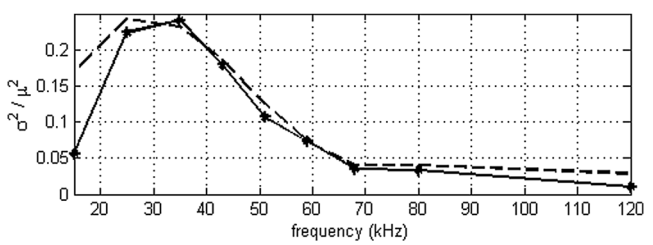

FIG. 7. The observed (stars) and predicted (dashed line) variance as a function of frequency. Note the variance has been normalized by the squared mean pressure.

Fig. 8 occurs at a frequency of 25 kHz for the highest void fraction, for which the standard deviation in the estimate of Eq. (8) is approximately 75% of the estimated value for Eq. (8). Elsewhere, the random uncertainty in the estimate of Eq. (8) is smaller, reaching a maximum of approximately 20%, 15%, and 10% of the estimate for Eq. (8), as the void fraction changes from 3.7×10^{-6} to 2.4×10^{-6} to 1.1×10^{-6}, respectively. It could also be that some portion of these deviations is due to an error in the calculation of Eq. (5), which is given only in approximate form by Eq. (7).

In order to examine the effect of bubble clustering, a modification was made to the bubble cloud generation system to generate statistical dependence in the positions of the bubbles. The honeycomb structure described earlier was removed, and approximately midway down the duct the circular cross-section was reduced to an approximately 10 cm diameter duct. A moveable nozzle of the same diameter was then placed on the end so that the flow of bubbles could be randomly redirected (by hand) to different locations throughout the course of an experiment. As the nozzle was moved from one direction to another, the number density of the bubbles in the first location was expected to diminish as the number density in the new location increased. The flow through the nozzle was estimated to be 15 cm/s, corresponding to a jet Reynolds number of 17 000, an indication that the flow through the nozzle was turbulent.

The spatial variation in the average bubble density (the single point statistic) was measured with the multibeam sonar using the same technique described earlier. The data look similar to those measured when the nozzle was not in place, although the variation in average bubble density in the cross-stream direction is slightly smaller, varying by no more than +/− 1 dB between the locations of the projector and the hydrophone.

The pair correlation function was also estimated from these data, as shown in Fig. 9. In contrast to the result from the nonclustered case shown in Fig. 3, the pair correlation function shown here is significantly higher than one for ranges less than 0.3 m indicating that there is structure present in the fluctuating bubble density. It is also interesting to note that the pair correlation does not asymptote to one at ranges greater than 0.3 m, but is instead less than one. This indicates that given the location of a bubble, it is less likely to find another bubble at distances greater than 0.3 m from the first bubble. This behavior is expected for the bubble cloud created with the nozzle: the fluctuating bubble density is always greater in the direction that the nozzle is pointed and lower where it is not pointed.

Multiple frequency acoustic propagation measurements were also collected through the bubble clouds generated with the moving nozzle, using the same methodology described earlier. The frequency dependent attenuation was extracted from the mean pressure field and inverted for the bubble size distribution, as shown in Fig. 10. A check of the inversion result was performed by using it to compute the attenuation that would be predicted from Eq. (1), and the result clearly matches the observation. If the assumption that clustering was not present in the bubble cloud were true, then the variance that would be predicted using the same bubble size distribution should match the observed variance. However, this turns out not to be the case for the data shown here where the observed variance is more than twice as high as the predicted variance between 43–80 kHz. This higher than expected variance is an indication that clustering is

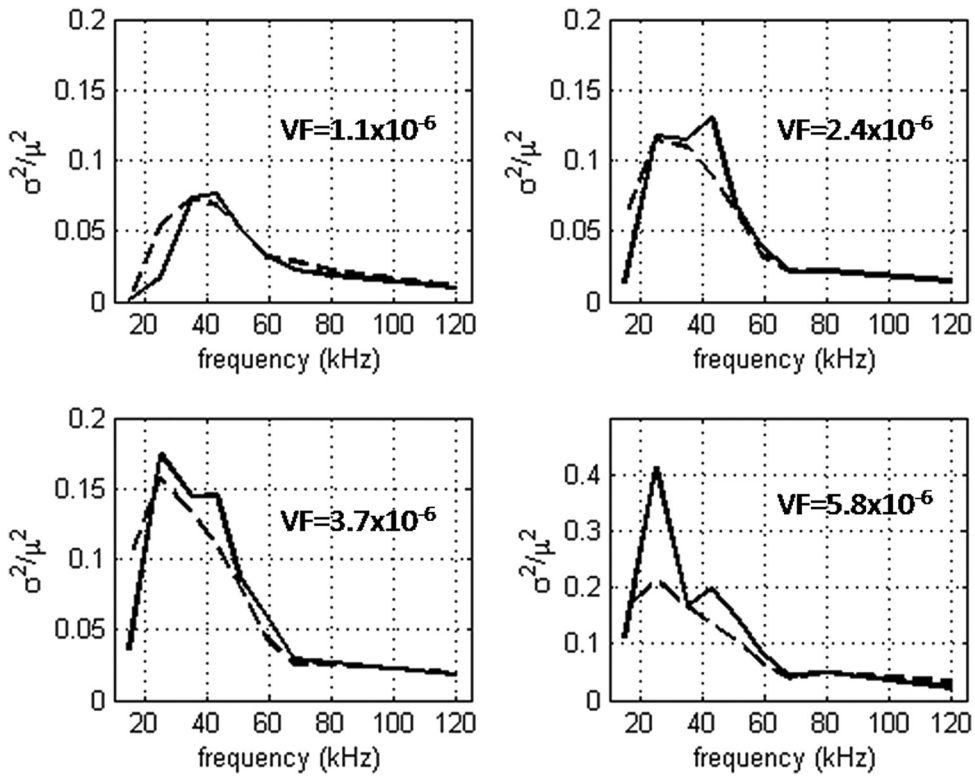

FIG. 8. A comparison between the observed (solid lines) and predicted (dashed lines) variance normalized by the squared mean pressure, plotted as a function of frequency for four different void fractions. The void fraction, VF, is shown for each of the four observations. Note that the vertical scale for the data on the lower right side is different from the other three plots.

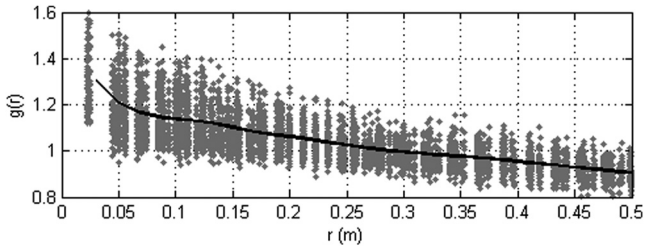

FIG. 9. An estimate of the pair correlation function for the bubble cloud generated with the moving nozzle.

present in the flow, invalidating the results of the inversion for the bubble size distribution.

When only single scattering is important, clustering should not have an impact on the acoustic measurements even when it is present. In order to investigate this, 75% of the ceramic bubble generators were removed from the laboratory apparatus used to generate the clustered bubble clouds, which had the effect of substantially reducing the number of bubbles exiting the moving nozzle. Three examples of the comparisons between observed and predicted variance are shown in the top row of Fig. 11 for void fractions of $1.3 \times 10^{-7} - 1.9 \times 10^{-7}$. Estimates of the standard deviation in Eq. (8) for these three examples are between 6%–7% of the estimated value for Eq. (8), with the exception of the estimate at 15 kHz for the third example (void fraction of 1.9×10^{-7}) in which the random error rises to almost 40%. Despite this outlier, the similarity between the predicted and observed variance indicate that the first and second moments are consistent and that bubble size distributions estimated from the frequency dependent attenuation data would be valid estimates. For the sake of comparison, three examples with higher void fractions ranging from $8.6 \times 10^{-7} - 1.1 \times 10^{-6}$ are shown in the bottom row of Fig. 11. Estimates of the random error in the Eq. (8) vary from $3\% - 7\%$ of the estimated value for Eq. (8). In each case, the observed variance is much higher than predicted variance, in contrast to

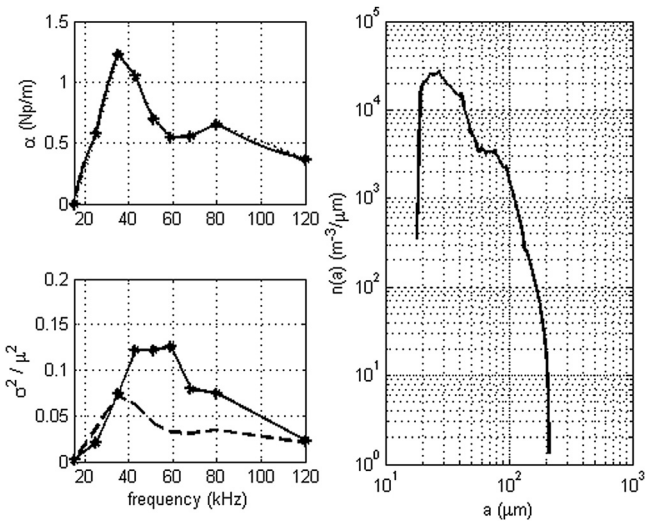

FIG. 10. The observed attenuation through the bubble cloud (upper left, stars) and the corresponding bubble size distribution estimated by inversion (right). The lower left shows the predicted (dashed line) and the observed (solid line) variance.

either the nonclustered or more tenuous bubble cloud cases. This is an indication that the inversion results and subsequent void fraction estimates are in error. Because the experimental procedure is essentially the same for all of the data shown in Fig. 11, with the exception of the quantity of bubble sources but including the presence of clustering, the difference between the top and bottom rows in Fig. 11 is thought to be associated with the transition from the single scattering case to the multiple scattering case.

IV. DISCUSSION

Clustering in bubble clouds has been previously shown to have a nonnegligible impact on acoustic fields (Weber *et al.*, 2007a; Weber, 2008). In the mean acoustic pressure field, these effects are present only when double scattering (or higher) chains contribute to the acoustic field in a significant way. In the case of inversions of multifrequency data for bubble size distributions this effect can be difficult to diagnose, particularly when only the average pressure field is examined. The results from these inversions, however, can be used to make predictions about the higher order statistical moments in the acoustic field, which in turn can be compared to the observations of these same statistics estimated from the same data set.

In this paper, comparisons between the predicted and observed 2nd moment were used as a metric to examine whether spatial clustering was present in the field of bubbles. These measurements were conducted for bubble distributions that are not dissimilar from that which would be observed under open ocean breaking waves. Further, the pair correlation function estimated for the clustered case in the laboratory setting described here was reasonably close to the pair correlation function that has been reported under open ocean breaking waves, at least at short distances [see Weber (2008), Fig. 6]. When clustering was imposed on the bubble field in the laboratory setting (as verified with the use of multibeam sonar measurements), the predicted and observed 2nd moments were shown to deviate by a factor of 2, far greater than our estimate of random error for the observation, providing an indication that the inversion was in error. Because the prediction is found using the average attenuation, which is a first moment quantity, this metric is really an examination of the consistency between the first and second moments.

In conducting the analysis described here, Foldy's one-way multiple scattering solution (Foldy, 1945) for the mean acoustic pressure field has been assumed to be correct and used as the basis for inversion of frequency dependent attenuation measurements for the bubble size distribution and subsequent estimates of the void fraction. It is possible that the neglected scattering terms in this solution have contributed to the inconsistency between the first and second moments for the observations of clustered bubble clouds at the higher void fractions. However, observations with consistent first and second moments have been made at void fractions that are nearly seven times greater than for the clustered bubble clouds. The void fraction estimates for the clustered bubble clouds are admittedly in error, meaning that this possibility

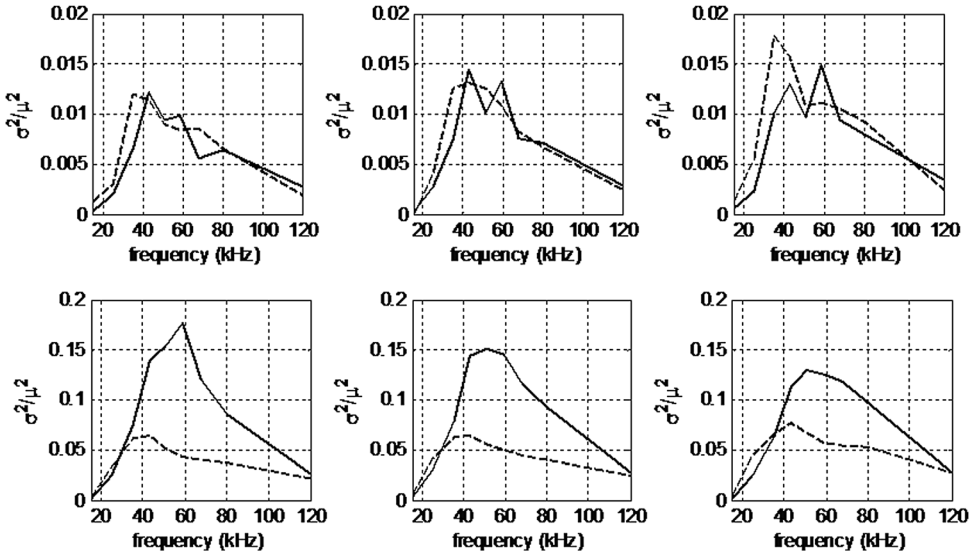

FIG. 11. A comparison between the observed (solid lines) and predicted (dashed lines) variance normalized by the squared mean pressure, plotted as a function of frequency for six different void fractions for clustered bubble clouds. The estimated void fractions (assuming clustering is not present) for the top row are 1.3×10^{-7}, 1.4×10^{-7}, and1.9×10^{-7} from left to right; for the bottom row they are 8.6×10^{-7}, 1.0×10^{-6}, and1.1×10^{-6} from left to right.

of an error in the inversion routine due to an incorrect theory for nonclustered bubble clouds cannot be concretely refuted, but this possibility seems unlikely in light of the collective measurements presented here. There will also be some error in the iterative, numerical inversion routine even with a perfect effective medium theory; analysis of this numerical error has not been undertaken as part of this work.

It has also been assumed that the shape of the bubble size distribution (i.e., the relative amount of bubbles of one size compared to another size) has been assumed to not vary in space or time. Due to their difference in size, however, bubbles may not respond identically when entrained in a turbulent flow. The research of Eaton and Fessler (1994) suggests that small particles may cross fluid flow streamlines depending on their Stokes number (the ratio of the response time of a bubble to some characteristic time scale in the fluid flow). Considering that the response time of a bubble is size dependent, it is possible that bubbles may selectively cross streamlines depending on their size. This would create statistical dependence between the size and location of multiple bubbles, a scenario which was not considered in this work but that could impact both the inversion result and the prediction for higher order moments.

The analysis described in this work assumed that the time series of observations collected for each scenario were stationary. Although this condition was strived for during the experiments, the data have not been conclusively shown to meet this condition, and this is an additional potential source of error in the results. In field settings (e.g., under breaking waves or in the bubbly wakes of ships), stationary data sets may be more difficult to acquire, and care should be taken to ensure that this is the case prior to examining the consistency between 1st and 2nd moments. It is also worth noting that because the frequency dependent attenuation and sound speed are linked via the dispersion relations (also known as the Kramers-Kroenig relations) (Arfken, 1985), the methodology presented here should be extendable to frequency dependent measurements of sound speed (e.g., Lamarre and Melville, 1995).

ACKNOWLEDGMENTS

The first author was supported by an NDSEG fellowship during the time these data were collected, for which he is grateful. The Applied Research Laboratory at Penn State generously provided the laboratory facilities used in the experiments described here. The comments and criticisms of the associated editor and three reviewers led to substantial improvements to the final manuscript, and were greatly appreciated. This work was supported by the Office of Naval Research Ocean Acoustics program (Code 321).

Arfken, G. (**1985**). *Mathematical Methods for Physicists,* 3rd ed. (Academic, New York), pp. 482–489.

Agrawal, Y. C., and Pottsmith, H. C. (**2000**). "Instruments for particle size and settling velocity observations in sediment transport," Mar. Geol. **168**, 89–114.

Barlow, J., Rae, Jr., W., and Pope, A. (**1999**), *Low-Speed Wind Tunnel Testing* (Wiley, New York), Chap. 3.

Caruthers, J. W., Elmore, P. A., Novarini, J. C., and Goodman, R. R. (**1999**). "An iterative approach for approximating bubble distributions from attenuation measurements," J. Acoust. Soc. Am. **105**, 185–189.

Coakley, C. R., Kane, T., Laux, A., Mullen, L., and J. Prentice, J. (**2002**). "Optical scattering measurements of bubble size distributions," *Ocean Optics XVI Conference*, Santa Fe, New Mexico, 18–22 November, 2002.

Commander, K. W., and Prosperetti, A. (**1989**). "Linear pressure waves in bubbly liquids: comparison between theory and experiments," J. Acoust. Soc. Am. **19**, 732–746.

Eaton, J., and Fessler, J. (**1994**). "Preferential concentration of particles by turbulence," Int. J. Multiphase Flow **20**, 169–209.

Fikioris, J., and Waterman, P. (**1964**). "Multiple scattering of waves. II. 'Hole corrections' in the scalar case," J. Math. Phys. **5**(10), 1413–1420.

Foldy, L. L. (**1945**). "The multiple scattering of waves, I. General theory of isotropic scattering by randomly distributed scatterers," Phys. Rev. **67**, 107–119.

Hahn, T. (**2007**). "Low frequency sound scattering from spherical assemblages of bubbles using effective medium theory," J. Acoust. Soc. Am. **122**(6), 3252–3267.

Henyey, F. (**1999**). "Corrections to Foldy's effective medium theory for propagation in bubble clouds and other collections of very small scatterers," J. Acoust. Soc. Am. **105**(4), 2149–2154.

Ishimaru, A. (**1978**). *Wave Propagation and Scattering in Random Media, Vol. II* (Academic, New York), Chap. 14.

Johnson, B., and Cooke, R. (**1979**). "Bubble populations and spectra in coastal waters, a photographic approach," J. Geophys. Res. **84**, 3761–3766.

Kargl, S. (**2001**). "Effective medium approach to linear acoustics in bubbly liquids," J. Acoust. Soc. Am. **111**(1),168–173.
Kinsler, L., Frey, A., Coppens, A., and Sanders, J. (**2000**). *Fundamentals of Acoustics*, 4th ed. (Wiley, New York), pp. 199.
Lamarre, E., and Melville, W. (**1995**). "Instrumentation for the measurement of sound speed near the ocean surface," J. Atmos. Ocean. Technol. 317–329.
Lax, M. (**1952**). "Multiple scattering of waves," Rev. Mod. Phys. **23**, 287–310.
Mallock, A. (**1910**). "The damping of sound by frothy liquids," Proc. R. Soc. London, Ser. A **84**, 391–395.
Medwin, H. (**1977**). "In situ acoustic measurements of bubbles at sea," J. Geophys. Res. **82**, 971–976.
Mehta, R., and Bradshaw, P. (**1979**). "Design rules for small low speed wind tunnels," Aeronaut. J. **83**, 443–449.
National Defense Research Committee. (**1946**). Physics of Sound in the Sea, Division 6 Summary Technical Report (National Defense Research Committee, Washington, DC), Vol. 8, pp. 441–546.
Novarini, J., Keiffer, R., and Norton, G. (**1988**). "A model for variations in the range and depth dependence of the sound speed and attenuation induced by bubble clouds under wind-driven seas," IEEE J. Ocean. Eng. **23**, 423–438.
Thorpe, S. (**1982**). "On the clouds of bubbles formed by breaking wind-waves in deep water and their role in air-sea gas transfer," Philos. Trans. R. Soc. London Ser. A **304**, 155–210.
Twersky, V. (**1953**). Multiple scattering of waves by a volume distribution of parallel cylinders, Research Report No. EM-59, Institute of Mathematical Sciences, New York University.
Van Wijngaarden, L. (**1972**). "One-dimensional flow of liquids containing small gas bubbles," Ann. Rev. Fluid Mech. **4**, 369–396.
Weber, T., Lyons, A. P., and Bradley, D. L. (**2007a**). "Acoustic propagation through bubble clouds exhibiting spatial structure in the fluctuating number density," IEEE J. Ocean. Eng. **32**(2), 513–523.
Weber, T. C., Lyons, A. P., and Bradley D. L. (**2007b**). "Identifying bubble clustering: comparisons of the coherent and incoherent fields," *Proc. 2nd Int. Conf. Underwater Acoustic Measurements: Technologies and Results*, Crete, Greece.
Weber, T. (**2008**). "Observations of clustering inside oceanic bubble clouds and the effect on short-range acoustic propagation," J. Acoust. Soc. Am. **124**(5), 2783–2792.
Ye, Z., and Ding, L. (**1995**). "Acoustic dispersion and attenuation relations in bubbly mixture," J. Acoust. Soc. Am. **98**(3), 1629–1636.